Electron beam echoes in the IOTA ring

Ben Luke[1]
SULI intern, FNAL

(Dated: 18 August 2023)

This study is a continuation of previous efforts to demonstrate the possibility of electron beam echo generation in the IOTA ring. Transverse beam echoes are conventionally produced by a dipole kick followed by a single quadrupole kick. We seek to use multiple quadrupole kicks over successive turns to generate an echo larger than that from a single kick. We use beam echo theory and simulations to model and predict the expected echo generated by multiple quadrupole kicks. We also run simulated scans over various parameters relevant to the echo to optimize the echo amplitude, including delay time, quadrupole strength, tune split, and pulse number. Effects due to quantum excitation and synchrotron damping (which are particularly relevant with electrons) were also considered in simulation. Results indicate that given sufficient quadrupole kick strength, we should expect to be able to measure electron beam echoes in the IOTA ring.

I. INTRODUCTION

The echo phenomenon has been observed in several areas of physics, not just particle beams. In fact, the discovery of echoes generally well precedes the observation of beam echoes. Spin echoes were first observed in 1950 by Hahn,[1] succeeded by the observation of photon echoes in 1964,[2] and the observation of plasma echoes in 1968.[3]

Echoes are generated by the application of a series of two "pulses" to the system. Depending on the type of system being observed, the term "pulse" will carry a different meaning. In the case of the spin echoes, pulses are applied in the form of intense radiofrequency power; for photon echoes, intense light pulses are applied, and for plasma echoes, electric fields. Similarly, the term "echo" carries a contextual meaning. For spin echoes, the echo is the reorienting of the spins in a common direction. For the photon echo this is a spontaneous burst of radiation, and for the plasma the echo is spatial. But in any case, the two calculated pulses result in the production of a spontaneous "echo," made possible by the intricate memory of phase space of the system.

The phenomenon of beam echoes is relatively new, though they were first observed more than three decades ago.[4] Analogous to the above cases, beam echoes are characteristically produced by the application of two magnetic "kicks" (i.e., pulses) to a beam of charged particles. The first kick is a dipole kick, initiating an initially coherent response that dies out due to phase mixing. Some time later, a quadrupole kick is applied, and the echo signal will follow. The echo here is a re-cohering of the beam to produce a sudden and pronounced amplification in the centroid signal. An example of a simulated echo is in Fig. 1.

Though an interesting phenomenon in its own right, the beam echo has useful properties relevant for accelerator science. Namely, beam echoes are particularly sensitive to diffusion, which is a measure of emittance growth. Diffusion measured in the traditional way takes on the order of hours; using the method of echoes would reduce the time several orders of magnitude. A quick measure of emittance growth will offer a quick test of beam stability.

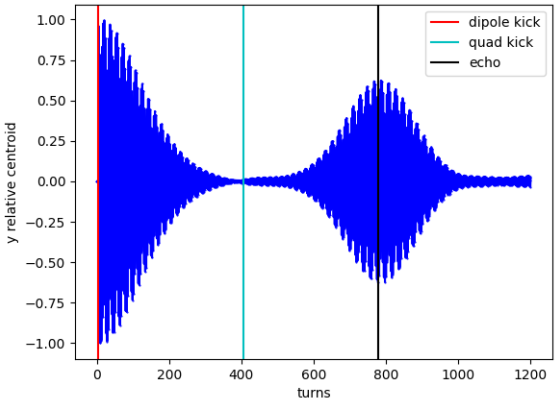

FIG. 1. Example of a beam echo. Note the initial dipole kick, followed by the quadrupole kick, followed by the echo signal. See also that the quadrupole kick does not affect the beam centroid. The y-axis is the centroid signal relative to the dipole kick.

If this method is successful, it can be extended to new intensity frontier hadron machines, such as the foreseen PIP-III rapid cycling synchrotron. Beyond beam stability measurements, echoes would allow the determination of better lattice configurations and the measurement of space-charge effects. A spectral analysis of the echo pulse can also be used to measure the tune shift from nonlinear forces in a synchrotron ring. Hence, beam echoes present themselves as a useful diagnostic tool and measurement device for the future of accelerator science.

Here at Fermilab, we are looking to use the Integral Optics Test Accelerator (IOTA) (see Fig. 2) to generate transverse electron beam echoes. Electron beam echoes would be novel, as it has been previously thought that the echo effect could not be observed in electron storage rings because of synchrotron radiation resulting in very strong diffusion. We seek to show that electron beam echoes are possible, so long as the decoherence time following the dipole kick is much shorter than the radiation damping time.

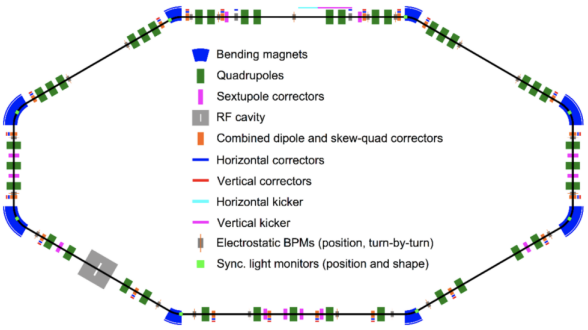

FIG. 2. Schematic of the IOTA machine. Note the dipole and quadrupole magnets for bending and focusing the beam, respectively, as well as nonlinear elements (sextupoles and octupoles) for beam correction. The sequence of elements in an accelerator or synchrotron is called a lattice.

The research in this paper primarily serves to address some issues presented with the generation of electron beam echoes in IOTA. One such issue deals with the quadrupole kicker strength. Owing to the fact that the quadrupole kicker strength is too weak at present to generate observable echoes, we seek to show that a larger signal can be generated by applying multiple quadrupole kicks over several turns. We also seek to optimize the number of kicks and the turn spacing between kicks in order to maximize the echo amplitude. Further, we consider the dependence upon quadrupole kick delay time following the initial dipole kick, quadrupole strength, and tune split, as well as effects from synchrotron damping and quantum excitation.

II. BEAM ECHO THEORY

Though a rigorous analysis of beam echo theory is outside the scope of this paper (more thorough treatments can be found elsewhere),[5,6] it will be useful to introduce some basics to lay a foundation for the motivation of this research. The brief introduction to linear beam echo theory in Section II A is adapted from Chao[5] and the work on multiple quadrupole kicks in Section II B is from Sen.[7]

A. Linear echo theory

Suppose we initially have a charged particle beam with initial emittance J_0, a Gaussian distribution in phase space resulting in an exponential distribution in the action variable J

$$\psi_0(J) = \frac{1}{2\pi J_0} e^{-J/J_0}, \tag{1}$$

and a betatron oscillation frequency that is amplitude dependent,

$$\omega(J) = \omega_0 + \omega' J, \tag{2}$$

where ω_0 is the nominal betatron frequency and ω' is the betatron detuning parameter. At time $t = 0$ we kick the beam with a dipole kicker to an amplitude $\beta\theta$, where β is the beta function at the dipole kicker and θ is the angle of deflection of the beam. The beam will then decohere due to phase mixing (i.e., different particles having slightly different oscillation frequencies). Once the beam has completely decohered and the centroid signal is zero, a quadrupole kick of strength q (defined $q \equiv \beta_Q/f$, where β_Q is the beta function at the quadrupole kicker and f is the focal length of the quadrupole) is applied, say at time $t = \tau$. This kick does not disrupt the beam centroid since the net force on the particles in the transverse plane is zero. Then the echo signal can be analytically represented as

$$\langle x\rangle(t) = \frac{\beta\theta q\omega' J_0\tau}{(1+\xi^2)^{3/2}} \sin(\Phi + 3\arctan(\xi)) \tag{3}$$

$$\xi = \omega' J_0(t - 2\tau), \tag{4}$$

$$\Phi = \omega_0(t - 2\tau). \tag{5}$$

The time-dependent amplitude can thus be described by the prefactor

$$\langle x\rangle^{\text{amp}}(t) = \frac{\beta\theta q\omega' J_0\tau}{(1+\xi^2)^{3/2}} \tag{6}$$

Given the factor of $1/(1+\xi^2)^{3/2}$, the amplitude will be small unless ξ^2 is small. Hence we expect to observe the echo greatest at $\xi = 0$, or $t = 2\tau$. This is a critical observation—a characteristic feature of the beam echo—that the centroid signal will recohere briefly at a time $t = 2\tau$ following the initial dipole kick. (Note that Eq. 3 represents *only* the echo signal; the amplification in the centroid signal due to the dipole kick that precedes is not modeled in this equation.)

B. Multiple quadrupole kicks

Conventionally beam echoes are made by only two pulses: a dipole kick followed by a quadrupole kick. However, with multiple quadrupole kicks it is possible to generate a larger echo than with only a single quadrupole kick. We can extend the ideas in Section II A to echo generation using multiple quadrupole kicks. Once again, we will only utilize the result; a full treatment can be found in the references.[7] The echo signal from N_q *additional* kicks in the linear regime can be expressed by

$$\langle x\rangle(t) = \beta\theta\omega' J_0 \sum_{m=0}^{N_q} q_m(\tau + mT_{\text{rev}}) \frac{\sin(\Phi_m + 3\arctan(\xi_m))}{(1+\xi_m^2)^{3/2}}, \tag{7}$$

$$\xi_m = \omega' J_0(t - 2(\tau + mT_{\text{rev}})), \tag{8}$$

$$\Phi_m = \omega_0(t - 2(\tau + mT_{\text{rev}})) \tag{9}$$

where m indexes the kick number, T_{rev} is the revolution period of the synchrotron, and the other variables are the

same as in Section II A. This formalism allows for varying kick strengths q_m, but in this paper we will assume a constant kick strength $q_m = q$ for all m. Under this assumption, Eq. 7 reduces to Eq. 3 when $N_q = 0$ (that is, one quadrupole kick), as expected.

C. Optimize N_q

By making use of Eq. 7, we can optimize the parameter N_q to maximize the echo. We used Mathematica to model the function numerically for various N_q. In Fig. 3 are models of echoes generated from $N_q = 0, 1, 2, 3$, whose amplitudes are relative to the max amplitude of a single quadrupole kick, $\beta\theta q\omega' J_0\tau$. What we find is that a value of $N_q = 1$, or two total consecutive-turn quadrupole kicks, generates the largest amplitude echo, with an improvement in amplitude of 57%. The model generated for $N_q = 2$ is comparable with a relative amplitude increase of 51%. The model for $N_q = 3$ is included to show that the benefits of additional kicks dies out quickly; here the relative amplitude decreases by 8.8%. This model is limited in insight since it is built only upon linear beam echo theory, but it will serve to give us an idea how many quadrupole kicks to apply in simulation to maximize the echo.

D. Quadrupole kick strength theory

Nonlinear theory of beam echoes predicts an amplitude dependence on the quadrupole strength q.[6] The theoretical model for small amplitude dipole kicks $\beta\theta \ll \sigma$ and quadrupole kicks $q \ll 1$ (which is usually well satisfied in practice), where σ is the rms beam size, is straightforward. The maximum amplitude relative to the initial dipole kick Q is predicted to reach a maximum of $Q_{\max} \approx 0.38$. The theoretical relationship between Q and q in these approximations is described by the equation

$$Q = q\tau T_{\rm rev}\omega' J\left[1 + \frac{1}{2}\left(\frac{\beta_k\theta}{\sigma}\right)^2\right]. \tag{10}$$

In this equation, τ is assumed to be measured in turns around the ring, though in formal theory τ has dimensions of time (hence the factor of $T_{\rm rev}$, the synchrotron revolution time). For IOTA, the parameters $T_{\rm rev} = 133.3$ ns and $J = 30$ nm are known, and we will assume here a delay time of $\tau = 400$ turns. Since this theory assumes a small dipole kick, we will be using it only as a very rough guide. We will assume a dipole kick of 22σ in these calculations, as well as in the following sections. To compute the optimal quadrupole kick strength $q_{\rm opt}$, we need only calculate ω', the detuning parameter, which can be described analytically as

$$\omega' = 2\pi f_{\rm rev}\frac{\Delta\nu_{\rm rms}}{J} \tag{11}$$

where $\Delta\nu_{\rm rms}$ is the rms tune shift $(\nu_0 - \nu_\sigma)_{\rm rms}$ between a particle traveling the nominal path with that of a particle traveling 1 rms beam size σ off the nominal path, and $f_{\rm rev}$ is the revolution frequency of the synchrotron. For IOTA, $f_{\rm rev} = 7500.6$ KHz. The rms tune shift was calculated using the MADX `DYNAP` module and was found to be $(\nu_0 - \nu_\sigma)_{\rm rms} = 3.7 \times 10^{-5}$. Calculating ω' is now straightforward and yields $\omega' = 5.8 \times 10^{10}$ (s-m)$^{-1}$. From these results, we obtain

$$q_{\rm opt} = 0.017.$$

It is worth making a note about the choice of dipole kick strength at 22σ. A smaller dipole kick would have been applied in practice if not for the fact that the decoherence time of the beam is quite sensitive to the dipole kick size. Gabriel shows in similar simulations that the decoherence time decreases with increased dipole kick size, and we find comparable behavior.[8] A longer decoherence time thus implies a longer delay time τ, since the quadrupole kick may only be applied once the centroid signal is zero. If we choose a longer delay time, however, problems arise from synchrotron radiation effects—which become more relevant at longer time scales—and will severely interfere with observation of electron beam echoes. These limitations considered, we have elected to use a larger dipole kick to keep the delay time short.

As already mentioned, the usefulness of this result is limited, as we have grossly deviated from the small dipole kick assumption of Eq. 10, but it will nevertheless serve as a rough guide and comparison as we scan q in Section III B.

III. SIMULATION

Following the modeling done using one-dimensional linear beam echo theory, we ran a series of simulations to more accurately identify the optimal sequence of quadrupole kicks, as well as to optimize various parameters relevant to echo production. Namely, we run scans over quadrupole kick strength, delay time, and tune split. To do the simulations, we use Methodological Accelerator Design (MADX) with a sequence code that models the lattice in IOTA. To analyze the MADX simulations, we use code written in C++, which outputs various data about the echo—most importantly, the maximum amplitude.

In Sections III C and III D we run scans over the delay time τ and tune split $\nu_y - \nu_x$, respectively. Among other parameters, we have chosen to keep the quadrupole kick strength $q = 0.0014$ constant. This choice of q was motivated by the experimental voltage limitations of the quadrupole kicker in IOTA. The currently achievable quadrupole voltage is expected at 140 V ($q = 0.0007$). Though no noticeable echo signal is observable at such a small voltage, simulations indicate that echoes can be observable if the quadrupole voltage increases by a factor of 2 (i.e., 280 V). Hence, our choice of $q = 0.0014$.

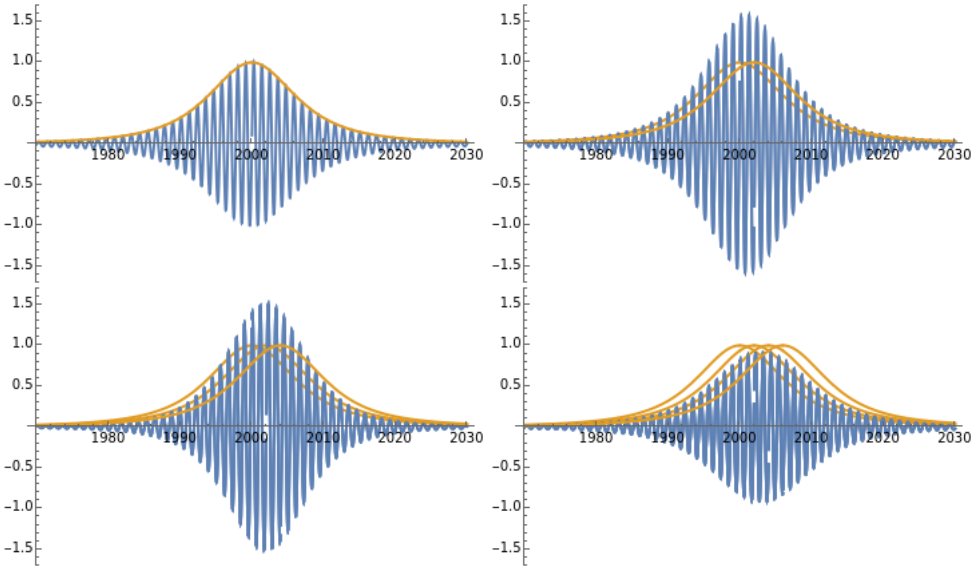

FIG. 3. Predictions of echoes for $N_q = 0, 1, 2, 3$ (left to right), respectively, using linear beam echo theory. The y-axis is the echo amplitude relative to the $N_q = 0$ echo maximum amplitude, $\langle x \rangle / (\beta\theta q \omega' J_0 \tau)$; the x-axis is the turn number. We have arbitrarily chosen a delay time of $\tau = 1000$ turns. The orange curves trace the amplitude contributions from each kick, which are all identical in shape since each kick is equal; they are only separated by a shift of one turn. Note that $N_q = 1$ yields the greatest echo amplitude, though $N_q = 2$ is a close second.

In these sections, we have also chosen to plot the echo signal above the background signal of the machine. We use the term "background signal" to denote centroid noise in the absence of any quadrupole kick. The choice to plot the subtracted echo signal (that is, the echo signal with background noise subtracted) was due to the small echo signal generated by a small quadrupole strength q. Note in other sections with larger q this was not necessary.

A. Quadrupole kick sequence

In the linear approximation modeling in Section II C, we assume additional quadrupole kicks are applied on successive turns. We need not restrict ourselves to this case, as we have the experimental liberty to delay the application of additional kicks by an integer number of turns. Previous work was done by Li that describes the sensitivity of the pulse sequence to the fractional tune of the machine.[9] This has to do with the "interplay between the timing of the pulse and the phase advance of the particles," as Li puts it. In other words, we would like to pulse the particles after the phase advance of the particles is an integer multiple of 2π, or very close. Given the fractional tune of IOTA at 0.3 ($\nu_{x,y} = 5.3$), we have chosen to narrow our search to sequences with pulse delays of 3 and 10 turns, in addition to consecutive turn pulses.

To be consistent with Li, we have chosen to represent a turn with a quadrupole kick (of positive polarity) with a p, and a turn with no kick with an x. Our convention, then, is to represent consecutive kicks with $pp \ldots p$, kicks that pulse every three turns with $(pxx)_{N_q}p$, and every ten turns with $(px_9)_{N_q}p$.

In simulation we find general agreement with the theoretical linear models in Section II C. From Fig. 4 we see that for the $pp \ldots p$ and $(px_9)_{N_q}p$ sequences, two total quadrupole kicks ($N_q = 1$) yields the greatest maximum relative amplitude. For the consecutive sequence pp we achieve an increase in maximum relative amplitude compared to the single kick of 11.4%; for six kicks every third turn $(pxx)_5 p$ an increase of 17.6%; and for two kicks separated by ten turns px_9p, a 20.8% increase. I qualify this statement by noting that there is some slight variation in optimal N_q that is dependent upon other factors like delay time τ and tune split. In some cases, $N_q = 2$ proved to be optimal in the $(px_9)_{N_q}p$ or consecutive-turn pulse sequence, but only marginally. Interestingly, however, for the $(pxx)_{N_q}p$ sequence, we find that the maximum echo amplitude almost always occurs at $N_q = 4$ or $N_q = 5$.

The maximum relative amplitude of the single quadrupole kick echo is 0.518, 36% greater than the predicted maximum relative amplitude from nonlinear theory $Q_{\max} \approx 0.38$. We should remind the reader, however, that this prediction assumes small quadrupole and dipole kicks, which we have not assumed in this section. We will apply small q in Sections III C and III D.

Of the sequences studied, we find the "ten sequence" $(px_9)_{N_q}p$ to yield the greatest amplitude echo at a relative maximum amplitude of 0.63 for $N_q = 1$. In the sections below, we have selected this sequence for analysis, unless otherwise noted, and we will compare its efficacy to that of only a single quadrupole kick.

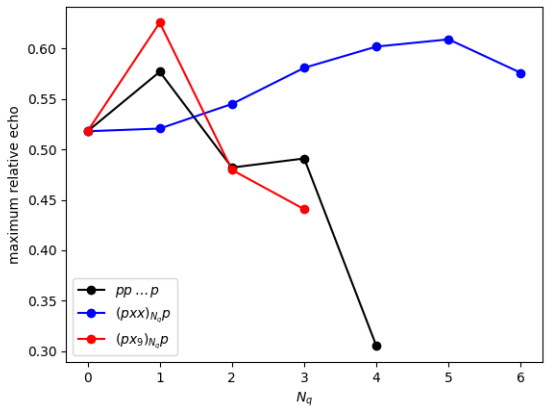

FIG. 4. Plot showing maximum relative echo amplitude from a simulated scan of three different sequences. The amplitude in this case is relative to the initial dipole kick. A delay time of $\tau = 400$ turns, dipole kick of 22σ, and tune split $\nu_y - \nu_x = 0.003$. The strength q of the quad kicker was varied to search for the maximum kick.

B. Scan over quadrupole strength q

A scan over the quadrupole strength q was done following the identification of the ten sequence as the best candidate (see Fig. 5). In these scans we have kept the tune split $\nu_y - \nu_x = 0.003$ and the delay time $\tau = 400$ turns constant. We did three scans: The first two are scans over two pulses, ten turns apart, one considering the effects due to quantum excitation and synchrotron damping, and another omitting the consideration of these effects. (These effects can be easily turned on or off in simulation by using the `DAMP` and `QUANTUM` attributes in MADX.) The third curve is a scan over q of only a single pulse. We find that $q = 0.047$ maximizes the amplitude for the blue curve (two pulses, ten turn separation) yielding a relative maximum amplitude of 0.625, a 20.6% improvement over the single kick whose maximum relative amplitude is 0.518 for $q = 0.049$. We note that these "optimal" quadrupole strengths are ~ 2.9 times larger than the predicted q_{opt} in Section II D. We attribute this to the large dipole kick at 22σ, where the theory applied above presupposes a small dipole kick. We also see rough agreement between the two blue plots—the curve that considers quantum excitation and damping effects generally traces the curve that does not consider these effects, even though the fine scale in Fig. 5 makes it look less obvious.

C. Scan over delay time

We also ran a scan over the delay time τ (Fig. 6). Here we have chosen to keep $q = 0.0014$ constant, so as to work in the $q \ll 1$ regime (see the earlier discussion in Section III for the motivation for the precise choice of q). Additionally, the parameters $\nu_y - \nu_x = 0.003$, and dipole kick of 22σ are constant.

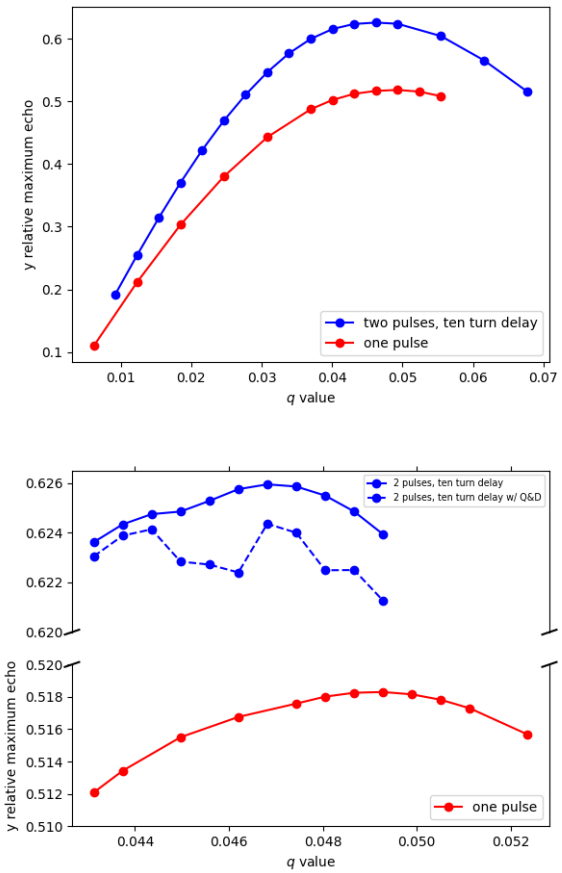

FIG. 5. Plots showing simulated scan over quadrupole strength q. The top plot is a more broad scan with courser scales. The bottom plot is a finer scan intended to narrow in on q_{opt}. The dashed blue curve is the scan done with two pulses, ten turns apart with quantum excitation and damping effects considered. For both plots, the solid blue curve is the same pattern but does not consider such effects; the red curve is the q scan over only a single quadrupole kick. We observe from the right plot that the optimum quadrupole strength q_{opt} shifts from 0.047 for the two pulse scheme to 0.049 for the single pulse scheme. A delay time of $\tau = 400$ turns, dipole kick of 22σ, and tune split $\nu_y - \nu_x = 0.003$ were constant. Note the broken axis on the plot on the right, adjusting the scales for each curve appropriately.

From Fig. 6 we find that the maximum echo (which is this time presented in terms of the subtracted background signal) from the ten sequence yields the largest amplitude echo. This echo has a relative maximum amplitude of 0.059, which is a 26% improvement from the relative maximum amplitude of the single kick echo. However, there is some variability in terms of which sequence performs the best for a given delay time. Nevertheless, we find that a delay time of 450 turns per-

forms the best overall, using two pulses separated by ten turns. We also plotted the same sequence of two pulses, separated by ten turns with quantum excitation and synchrotron damping (Q&D) effects considered (dashed blue line), to verify our initial simulations omitting such effects (solid blue line). We see that these lines are almost identical, assuring us that Q&D effects are less relevant in our current setup.

Unfortunately, however, even our best echo in this analysis is orders of magnitude off from the much larger echoes in Section III B. Though it is possible we observe larger echoes at longer delay times (as Gabriel showed),[8] we have kept our scan of delay times within a fairly limited range of relatively short τ to avoid experiencing damping effects, as discussed in Section II D. (In IOTA, the damping time is[10] 0.65 s or 4.9×10^6 turns, so operating at $300 \leq \tau \leq 600$ turns is well under that time.) The agreement between the Q&D and non-Q&D plots in Fig. 6 further verifies that we have selected a delay time τ sufficiently smaller than the radiation damping time.

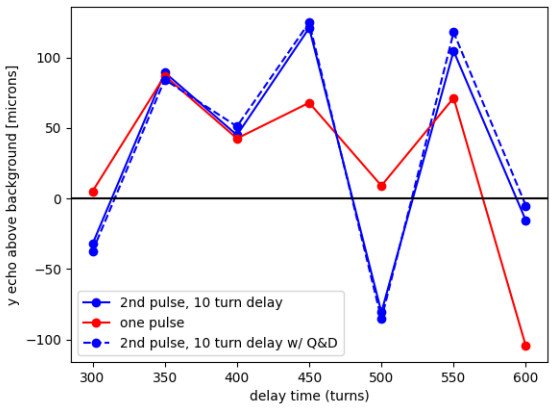

FIG. 6. Plot showing simulated delay time scan from 300 to 600 turns in 50 turn intervals. The solid blue line indicates two pulses, separated by ten turns, without the consideration of quantum excitation and synchrotron damping (Q&D) effects; the dashed blue line is the same sequence that does consider Q&D effects; the red line is only a single pulse, without consideration of Q&D effects. The y-axis is the echo signal (in μm) above the background signal. We find a maximum echo at 450 turns. The simulation was ran with a tune split of $\nu_y - \nu_x = 0.003$ and $q = 0.0014$.

Note that we have also chosen to plot the echo signals in Fig. 6 as the centroid distance *above* the background signal, which otherwise overwhelms the echo signal rendering it largely unnoticeable. Fig. 7 shows the same echo, one without any background noise subtractions and one with background subtractions ("background" noise was generated by setting $q = 0$ and running the simulation). It is obvious from the plots in Fig. 7 that background noise can significantly drown out the detection of the echo, as well as disguise the echo's "true" location. In the case of the left-hand plot, the echo's peak is measured at 963 turns, but on the right-hand plot it is centered precisely where expected at $t = 905$ turns (the offset of 5 turns results from the dipole kick at $t = 5$ turns).

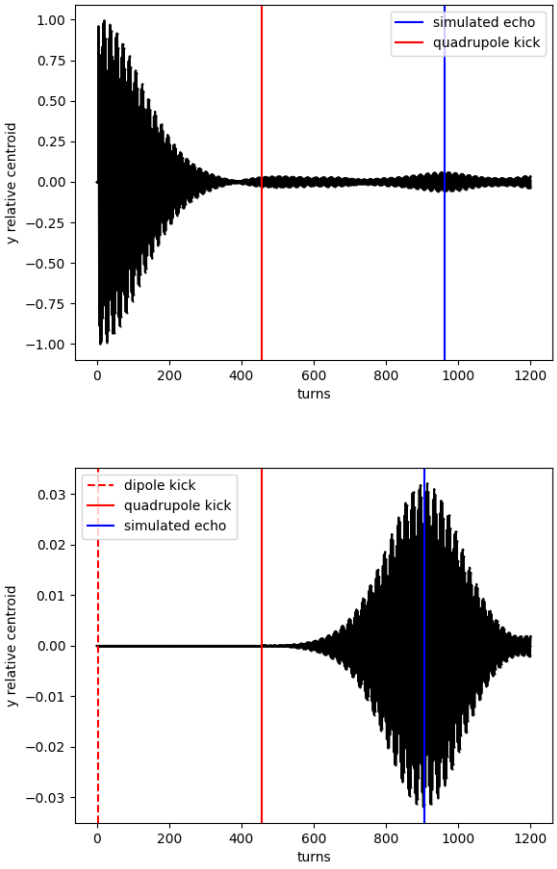

FIG. 7. Top: Simulation of echo with $q = 0.0014$, $\tau = 450$ turns, $\nu_y - \nu_x = 0.003$, and a dipole kick of 22σ. Bottom: Same echo with background noise subtracted (including dipole kick signal) and scaled to the frame size. This shows visually the effects of the background signal for small amplitude beam echoes. We also see from the right hand plot that the echo signal is centered precisely at the expected time $t = 905$ turns, as expected (the dipole kick is initiated at $t = 5$ turns).

D. Transverse coupling

The effects due to transverse coupling were considered by scanning over the tune split. Transverse coupling implies that beam dynamics in one plane will have effects on the other plane—coupling is greatest when $\nu_y = \nu_x$. Hence, coupling can have implications for the production of echoes and will affect the amplitude. In our scan we used the same parameters as in Section III C, with the obvious change that the tune split is varied and here we hold the delay time constant at 400 turns.

The scan in Fig. 8 compares the echo amplitude above the background signal from a two pulse setup (10 turn pulse delay) and from a single pulse. Again, we have somewhat mixed results, comparable to the analysis in Section III C. What we find is that the largest amplitude echo with a relative maximum of 0.11 is produced from the two pulse scheme with a tune split of $\nu_y - \nu_x = 0.018$. This is an improvement of 27% over the single kick. However, the two pulse sequence does not always outperform the single kick scheme, and we find that at particular tune splits the single kick yields a better echo than two kicks.

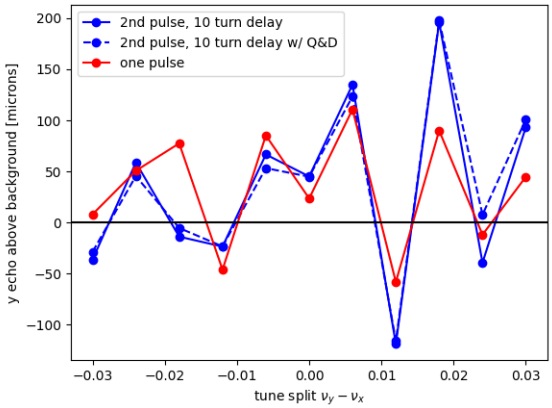

FIG. 8. Plot showing simulated tune split scan. The blue line indicates two pulses, separated by ten turns; the red line is only a single pulse. The y-axis is the echo signal (in μm) above the background signal. We find a maximum echo amplitude at a tune split of 0.018. The simulation was run with delay time $\tau = 400$ turns and $q = 0.0014$.

IV. DISCUSSION AND CONCLUSION

The purpose of this paper is to analyze the possibility of using multiple successive quadrupole kicks in the IOTA to generate a larger echo signal than that generated by only a single quadrupole kick. We first showed this to be theoretically true in the linear limit, identifying $N_q = 1$ to be the optimal number of kicks for generating a large echo, offering a 57% improvement over the single kick amplitude. This, however, was only for consecutive turn kicks.

In simulation we then considered many different numbers and patterns of quadrupole kicks, informed by the fractional tune of IOTA. Three viable candidates were selected and tested in simulation. What we found is that the application of 2 kicks separated by ten turns generated the largest echo. In the scan over quadrupole strength, we observe an echo amplitude dependence that grows with quadrupole strength to a value q_{opt} but then begins to decay. This shape is similar to what is expected from nonlinear theory of both dipole and quadrupole strength.[6] We also see only a 4% difference between the q_{opt} values for the one and two pulse schemes. This is unfortunate from an experimental standpoint, since our maximum quadrupole kicker strength is much smaller than this (around $q = 0.0014$, at best). Further, at $q < q_{\text{opt}}$ the benefit of two pulses compared to one becomes marginal, with all other parameters constant (see Fig. 5).

For scans in the small quadrupole kick regime (we used $q = 0.0014$ corresponding to an experimental quadrupole voltage supply of 280 V) echo amplitude showed variable dependence upon both delay time and tune split. Nevertheless, according to the scope of the scans we performed we find a maximum echo with a delay $\tau = 400$ turns and tune split $\nu_y - \nu_x = 0.018$, which generated an improvement of 27% when compared to the maximum relative echo amplitude generated by only a single quadrupole kick. Compare the maximum amplitude echo generated by only a single pulse to that of the maximum amplitude echo generated by two pulses, ten turns apart (Fig. 9).

The same scans were also done considering the effects of synchrotron radiation damping and quantum excitation, but showed negligible difference when compared to scans that did not consider such effects. This indicates that these effects are not relevant at the small delay times we have selected. Comparisons with nonlinear echo theory were made, but few insights were offered due to the fact that the nonlinear theory used assumed small dipole kicks—we were unable to meet these assumptions in our simulations. This can be corrected by comparing the simulations with the more complete nonlinear dipole and quadrupole theory presented in Sen and Li.[6]

It is important to note that this project is still ongoing, with more simulations being run (and repeated) as we gain information about experimental hardware limitations (such as quadrupole kicker strength) and as we optimize other parameters within the IOTA lattice (such as nonlinear elements). As we look towards experiment, we will likely have to find a means of improving the quadrupole kicker strength. The resolution of the beam position monitor (BPM) will also have to be improved if kicker strength limitations still remain, down to the order of a few microns.

V. ACKNOWLEDGEMENTS

I am indebted to many people for the work presented in this paper. Above all I would like to express my gratitude to my research mentor, Tanaji Sen, for his supervision, instructive feedback, and patience during the project. In addition, many thanks are due to Francois Ostiguy for his volunteered communication, helpful instruction, and other contributions to the work this summer. I am grateful also to Jonathan Jarvis for his leadership and and technical input during the project, as well as for his lab hospitality that facilitated a positive and productive work

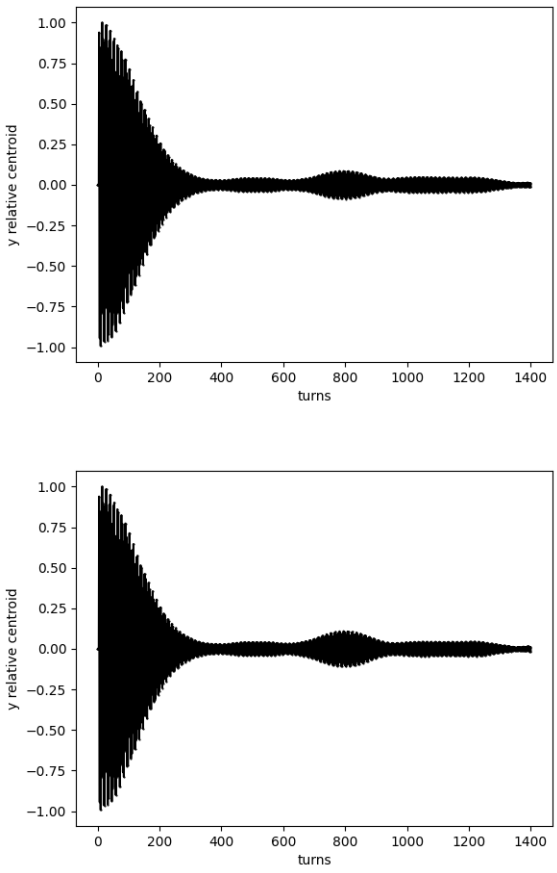

FIG. 9. Simulated echo showing the signal from only a single kick (left) to the signal from two kicks separated by ten turns. Both were generated with $q = 0.0014$, tune split $\nu_y - \nu_x = 0.018$, delay $\tau = 400$ turns, and dipole kick of 22σ.

environment.

Others, though less immediately involved, have also been valuable influences in this research. Thanks to Judy Nunez for her flexibility during the production of the report. Thanks also to Phill Broussard and Don Petcher for their substantial support, encouragement, and training in my development as a student researcher. Lastly, I am always indebted to my family for the ways in which they support my success both holistically in my various endeavors and also particularly in my scientific pursuits.

[1] E. L. Hahn. Spin echoes. *Phys. Rev.*, 80(4):580, 1950.
[2] N. A. Kurnit, I. D. Abella, and S. R. Hartman. Observation of a photon echo. *Phys. Rev. Lett.*, 13(19):567, 1964.
[3] R. W. Gould and t. M. O'Neil. Observation of plasma wave echoes. *Phys. Fluids*, 11(6):1147, 1968.
[4] L. K. Spentzouris, J-F. Ostiguy, and P. L. Colestock. Measurement of diffusion rates in high energy synchrotrons using longitudinal beam echoes. *Phys. Rev. Lett.*, 76:620, 1996.
[5] A. W. Chao. Lecture notes: Echoes. `www.slac.stanford.edu/~achao/lecturenotes.html`.
[6] Tanaji Sen and Yuan Shen Li. Nonlinear theory of transverse beam echoes. *Phys. Rev. Accel. Beams*, 21:021002, Feb 2018.
[7] Tanaji Sen. Echoes notes. Fermilab TM.
[8] Annika Gabriel. Investigation of beam echo generation with electrons in the iota ring. Technical report, Case Western Reserve University, 2019.
[9] Yuan Shen Li. Diffusion measurement with transverse beam echoes. Technical report, Carlton College, 2017.
[10] A. Romanov, J. Santucci, and G. Stancari. Experimental Single Electron 4D Tracking in IOTA. 7 2023.